Protein Science (2000), *9*:49–52. Cambridge University Press. Printed in the USA.

Crystal structures of two mutants (K206Q, H207E) of the N-lobe of human transferrin with increased affinity for iron

AMY H.-W. YANG,[1] ROSS T.A. MacGILLIVRAY,[1] JIE CHEN,[1] YAOGUANG LUO,[1] YILI WANG,[1] GARY D. BRAYER,[1] ANNE B. MASON,[2] ROBERT C. WOODWORTH,[2] AND MICHAEL E.P. MURPHY[1,3]

[1]Department of Biochemistry & Molecular Biology, University of British Columbia, Vancouver, British Columbia V6T 1Z3, Canada
[2]Department of Biochemistry, University of Vermont, Burlington, Vermont 05405-0068
[3]Department of Microbiology and Immunology, University of British Columbia, Vancouver, British Columbia V6T 1Z3, Canada

(Received June 29, 1999; Final Revision October 5, 1999; Accepted October 6, 1999)

Abstract

The X-ray crystallographic structures of two mutants (K206Q and H207E) of the N-lobe of human transferrin (hTF/2N) have been determined to high resolution (1.8 and 2.0 Å, respectively). Both mutant proteins bind iron with greater affinity than native hTF/2N. The structures of the K206Q and H207E mutants show interactions (both H-bonding and electrostatic) that stabilize the interaction of Lys296 in the closed conformation, thereby stabilizing the iron bound forms.

Keywords: crystal structure; human transferrin; iron; mutant

The transferrins are a group of iron-binding proteins that have a high affinity ($K_d = 10^{-23}$ M) for ferric iron (Baker et al., 1994). While serum transferrin transports Fe(III) to cells where the Fe(III) is taken up via the ubiquitous transferrin receptor (Aisen, 1998), the ovotransferrins and lactoferrins are thought to play antimicrobial roles by limiting the availability of Fe(III) required for growth (Baker et al., 1994). Structural studies of human lactoferrin and transferrin have shown that these proteins are comprised of two lobes joined by a bridging peptide; each lobe is comprised of two domains that form a cleft containing a high-affinity binding site for Fe(III) and other transition metals (Baker et al., 1994). The Fe(III) is bound in a distorted octahedral coordination to four protein ligands (in human transferrin N-lobe by Asp63, Tyr95, Tyr188, and His249) and two ligands from a synergistically bound, bidentate anion. Iron release occurs in a pH- and receptor-dependent process by the rotation and opening of the domains around a hinge (see Baker et al., 1994; Aisen, 1998, for recent reviews).

By using recombinant DNA techniques, the N-lobe of human transferrin (hTF/2N) has been expressed at high levels in both mammalian tissue culture cells (Funk et al., 1990) and the yeast *Pichia pastoris* (Steinlein et al., 1995; Mason et al., 1996). X-ray crystallographic studies have revealed that these recombinant forms of hTF/2N (MacGillivray et al., 1998; Bewley et al., 1999) have the same polypeptide folding as rabbit serum transferrin (Bailey et al., 1988). However, the presence of a single metal-binding site in hTF/2N simplifies the kinetic analysis of metal binding and release when compared to serum transferrin. Using in vitro mutagenesis, several point mutations of hTF/2N have been expressed and characterized including ligating residues (Woodworth et al., 1991; Zak et al., 1995; He et al., 1997a, 1997b; Mason et al., 1998), second shell residues (Woodworth et al., 1991; He et al., 1998), a pair of lysine residues that have been implicated (Dewan et al., 1993) in iron release via a dilysine trigger (Li et al., 1998; Steinlein et al., 1998; He et al., 1999), and other functional residues (Luck et al., 1997; Zak et al., 1997). Spectral and kinetic analyses of these mutant forms of hTF/2N have shown that it is possible to manipulate the iron binding characteristics of hTF/2N so that it binds iron more or less tightly than wild-type hTF/2N (Woodworth et al., 1991; Lin et al., 1993; Li et al., 1998; Steinlein et al., 1998). Although the X-ray crystal structures of Fe(III)-hTF/2N (MacGillivray et al., 1998) and apo-hTF/2N (Jeffrey et al., 1998) have been reported, the structural changes associated with the introduction of point mutations in hTF/2N have not been determined. In this paper, we report high-resolution crystal structures of two mutants of hTF/2N–K206Q and H207E. These are the first mutant structures of hTF/2N to be determined and provide an explanation for the higher iron-binding affinity of these mutants relative to wild-type hTF/2N.

Reprint requests to: Michael E.P. Murphy, Department of Microbiology and Immunology, University of British Columbia, #300 6174 University Boulevard, Vancouver, British Columbia V6T 1Z3, Canada; e-mail: memurphy@interchange.ubc.ca.

Results and discussion

The overall folding of the polypeptides of the K206Q and H207E mutants is very similar to that found for native Fe(III)-hTF/2N (MacGillivray et al., 1998). When the structures of the mutants were superimposed with the native hTF/2N structure using the program Xtalview (McRee, 1992), no significant deviations were observed among the main-chain atoms (RMS deviation for main-chain atoms is 0.13 Å for both mutants). In addition, strong electron density was observed for the iron atom; this is consistent with the orange-red color of both of the crystals used for data collection. However, local changes around the mutated residue were found as shown in Figure 1, and discussed below.

K206Q

In native hTF/2N, Lys206 NZ forms an unusual H-bond to Lys296 NZ (Fig. 1A), which constitutes the dilysine trigger (Dewan et al., 1993; MacGillivray et al., 1998). In the structure of K206Q hTF/2N, the conformation of the Gln206 side chain is similar to that of the wild-type lysine, resulting in Gln206 OE1 being located 2.9 Å from Lys296 NZ, allowing for a hydrogen bond to be retained between these residues (Fig. 1B). This H-bond is maintained by a small displacement of 0.43 Å by the NZ atom of Lys296 in the mutant relative to native hTF/2N structure. The side-chain amide of Gln206 is within H-bonding distance to two solvent atoms (Wat354 and Wat350) that are conserved in position in the native protein.

In the crystallographic model, it is possible that the conformation of the Gln206 side-chain amide is flipped, resulting in the approximate exchange in the positions of the OE1 and NE2 atoms. The conformation shown in Figure 1B was chosen on the basis of obtaining slightly lower overall *R*-factors and more similar *B*-factors for the affected atoms. In addition, interaction of the oxygen of a side-chain amide with a lysyl amine allows for Lys296 to be protonated; however, presumably either Lys206 or Lys296 is not protonated at neutral pH in the dilysine trigger. Additional experiments will be required to confirm the nature of the H-bond interaction between Gln206 and Lys296.

The removal of iron from K206Q hTF/2N requires more extreme conditions of low pH (<4.0) compared to the native protein (pH 5) (Woodworth et al., 1991). Furthermore, calorimetric stud-

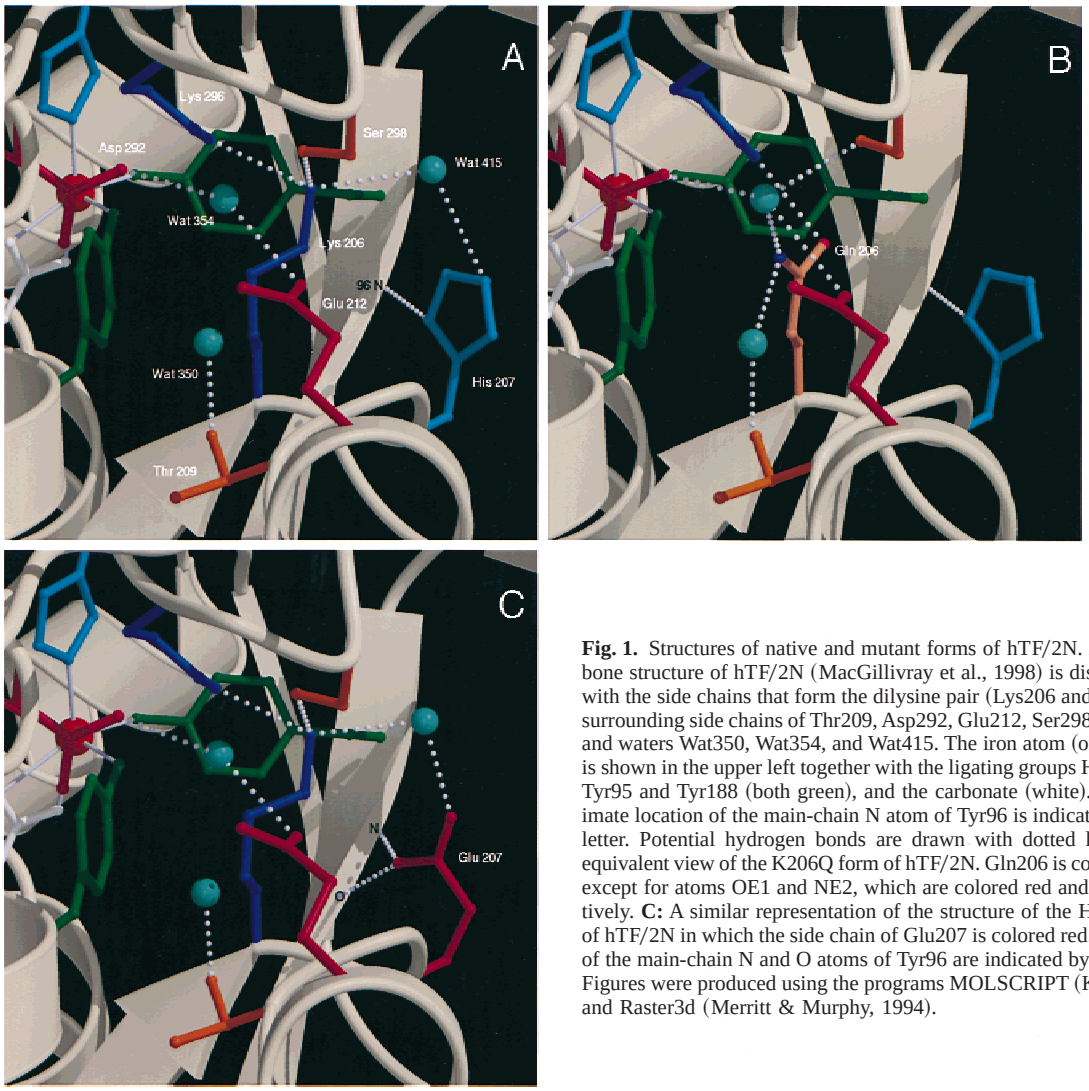

Fig. 1. Structures of native and mutant forms of hTF/2N. **A:** The backbone structure of hTF/2N (MacGillivray et al., 1998) is displayed along with the side chains that form the dilysine pair (Lys206 and Lys296), the surrounding side chains of Thr209, Asp292, Glu212, Ser298, and His207, and waters Wat350, Wat354, and Wat415. The iron atom (orange sphere) is shown in the upper left together with the ligating groups His249 (blue), Tyr95 and Tyr188 (both green), and the carbonate (white). The approximate location of the main-chain N atom of Tyr96 is indicated by a black letter. Potential hydrogen bonds are drawn with dotted lines. **B:** The equivalent view of the K206Q form of hTF/2N. Gln206 is colored salmon, except for atoms OE1 and NE2, which are colored red and blue, respectively. **C:** A similar representation of the structure of the H207E mutant of hTF/2N in which the side chain of Glu207 is colored red. The location of the main-chain N and O atoms of Tyr96 are indicated by black letters. Figures were produced using the programs MOLSCRIPT (Kraulis, 1991) and Raster3d (Merritt & Murphy, 1994).

ies suggest that iron binding by this mutant is 20-fold tighter than for hTF/2N (Lin et al., 1993). In the structure of the apo-hTF/2N, Asp63 forms a H-bond with Lys296 indirectly orienting the His249 iron ligand (Jeffrey et al., 1998). In the K206Q mutant, the H-bond between Gln206 and Lys296 may be retained at lower pH preventing the reorganization of the H-bond network in the apo-form and favoring the iron bound form. The stability of the interaction of Gln206 with Lys296 is supported by the low *B*-factors observed for this residue in the mutant structure (17.3 Å^2).

H207E

In the structure of native Fe(III)-hTF/2N, the imidazole side chain of His207 forms an H-bond with the main chain of Tyr96, a residue adjacent to the iron ligand Tyr95, and an electrostatic interaction with Lys206 NZ (Fig. 1A). The replacement of His207 with glutamate alters these interactions (Fig. 1C). The Glu207 side chain forms an H-bond to Lys206 NZ via an equivalent bridging water molecule (Wat415). The other oxygen of the side-chain carboxylate forms H-bonds to the main-chain atoms of Tyr96.

The close proximity of His207 to the dilysine trigger in the native structure of hTF/2N suggests that this residue may influence iron-binding properties. The presence of a negative charge resulting from the H207E mutation would be expected to stabilize the dilysine trigger favoring the iron bound form. In fact, the H207E mutant binds ferric iron more tightly than native hTF/2N (Woodworth et al., 1991; Lin et al., 1993), and iron release is kinetically slower (Zak et al., 1995). The *B*-factors of the Glu207 side chain (17.6 Å^2) are significantly lower than the structure average (27.6 Å^2).

In summary, the structures of the mutations K206Q and H207E show that the dilysine pair plays a key role in determining the iron affinity of the N-lobe of human transferrin. The structures show that the mutated side chains stabilize Lys296 in the iron bound structure, thereby leading to stabilized iron-binding sites.

Materials and methods

Expression and crystallization of mutant proteins

Details of the construction of the H207E and K206Q mutants of hTF/2N, and their subsequent expression in baby hamster kidney cell lines, have been described previously (Woodworth et al., 1991). Crystals were obtained by the hanging drop method at 4 °C by mixing equal amounts of reservoir solution with the hTF/2N mutant protein (40 mg/mL in 40 mM sodium cacodylate buffer pH 5.75). The reservoir solution contained 26% polyethylene glycol 4000 and 20 mM sodium bicarbonate. Colored crystals were obtained for both the K206Q and H207E mutants, suggesting that the Fe(III)-bound forms had been crystallized. Both mutant forms of hTF/2N crystallized isomorphously with the wild-type protein in space group $P2_12_12_1$ with one molecule in the asymmetric unit (Wang et al., 1992).

Data collection and refinement

For each mutant protein, a complete data set was collected from a single crystal using a Rigaku R-Axis IIc image plate system. Incident X-rays were generated from a rotating anode generator operating at 59 kV and 90 mA and passed through a graphite monochromator. The X-ray diffraction data were processed using the computer programs DENZO and Scalepack (Otwinowski & Minor, 1997). The H207E mutant diffraction data were processed to 2.0 Å resolution, while the K206Q diffraction set was processed to a resolution of 1.8 Å.

Table 1. *Data collection and refinement statistics for the two mutants of hTF/2N*

	K206Q	H207E
Cell dimensions (Å)	a = 45.01, b = 57.81, c = 135.6	a = 45.03, b = 57.91, c = 135.9
Resolution (Å)	1.8	2.0
R_{merge} on I	0.069 (0.284)[a]	0.043 (0.130)
$\langle I\rangle/\langle\sigma(I)\rangle$	15.3 (3.7)	20.1 (7.9)
Completeness (%)	91 (96)	88 (89)
Unique reflections	30,624 (3,159)	21,745 (2,165)
Redundancy	2.9 (2.8)	2.9 (2.6)
Working *R*-factor	0.184 (0.295)	0.179 (0.249)
Free *R*-factor	0.225 (0.309)	0.218 (0.260)
RMS deviation from ideal geometry		
Bond length (Å)	0.008	0.009
Bond angles (Å)	1.41	1.34
Number of solvent atoms	139	135

[a]Values in parentheses are for the highest resolution shell.

The mutant structures were solved by molecular replacement using the coordinates for the orthorhombic crystal form of Fe(III)-hTF/2N (MacGillivray et al., 1998) as the starting model, except that the mutated residue was changed to an alanine residue, and surrounding water molecules were removed. Simulated annealing, positional, and *B*-factor refinement was carried out using the program X-PLOR (Brünger, 1990). Initially, the mutant side chain was inserted manually using the program Xtalview (McRee, 1992). Additional water molecules were added by searching $F_o - F_c$ maps and were screened for appropriate *B*-factors, H-bonds, and electron density in σ_a-weighted $2F_o - F_c$ maps. Table 1 provides a summary of final refinement statistics for each mutant structure. As defined by the program PROCHECK (Laskowski et al., 1993), greater than 86% of the residues of the two mutant structures are in the most favored region in Ramachandran plots. Two residues are in the disallowed region, Lys4 and Leu294; the latter is found in a γ-turn characteristic of the transferrin and lactoferrin structures (see MacGillivray et al., 1998). Detailed data processing and refinement statistics for both mutants are given in Table 1.

Acknowledgments

This work was supported by MRC of Canada operating grants to M.E.P.M. and R.T.A.M. (MT-14767), and to G.D.B. (MT-13338), and by a USPHS Grant (R01 DK 21739) to R.C.W. M.E.P.M. is the recipient of a MRC scholarship.

References

Aisen P. 1998. Transferrin, the transferrin receptor, and the uptake of iron by cells. *Metal Ions Biol Syst 35*:585–631.

Bailey S, Evans RW, Garratt RC, Gorinsky B, Hasnain S, Horsburgh C, Jhoti H, Lindley PF, Mydin A, Sarra R, et al. 1988. Molecular structure of serum transferrin at 3.3-Å resolution. *Biochemistry 27*:5804–5812.

Baker EN, Anderson BF, Baker HM, Day CL, Haridas M, Norris GE, Rumball SV, Smith CA, Thomas DH. 1994. Three-dimensional structure of lactoferrin in various functional states. *Adv Exp Med Biol 357*:1–12.

Bewley MC, Tam BM, Grewal J, He S, Shewry S, Murphy MEP, Mason AB, Woodworth RC, Baker EN, MacGillivray RTA. 1999. X-ray crystallography and mass spectroscopy reveal that the N-lobe of human transferrin expressed in *Pichia pastoris* is folded correctly but is glycosylated on serine-32. *Biochemistry 38*:2535–2541.

Brünger AT. 1990. *X-PLOR, version 3.1*. New Haven, Connecticut: Yale University.

Dewan JC, Mikami B, Hirose M, Sacchettini JC. 1993. Structural evidence for a pH-sensitive dilysine trigger in the hen ovotransferrin N-lobe: Implications for transferrin iron release. *Biochemistry 32*:11963–11968.

Funk WD, MacGillivray RTA, Mason AB, Brown SA, Woodworth RC. 1990. Expression of the amino-terminal half-molecule of human serum transferrin in cultured cells and characterization of the recombinant protein. *Biochemistry 29*:1654–1660.

He QY, Mason AB, Tam BM, MacGillivray RTA, Woodworth RC. 1999. The dual role of Lys 206–Lys 296 interaction in human transferrin N-lobe: Iron release trigger and anion-binding site. *Biochemistry 38*:9704–9711.

He QY, Mason AB, Woodworth RC, Tam BM, MacGillivray RTA, Grady JK, Chasteen ND. 1997a. Inequivalence of the two tyrosine ligands in the N-lobe of human serum transferrin. *Biochemistry 36*:14853–14860.

He QY, Mason AB, Woodworth RC, Tam BM, MacGillivray RTA, Grady JK, Chasteen ND. 1998. Mutations at nonliganding residues Tyr-85 and Glu-83 in the N-lobe of human serum transferrin. Functional second shell effects. *J Biol Chem 273*:17018–17024.

He QY, Mason AB, Woodworth RC, Tam BM, Wadsworth T, MacGillivray RTA. 1997b. Effects of mutations of aspartic acid 63 on the metal-binding properties of the recombinant N-lobe of human serum transferrin. *Biochemistry 36*:5522–5528.

Jeffrey PD, Bewley MC, MacGillivray RTA, Mason AB, Woodworth RC, Baker EN. 1998. Ligand-induced conformational change in transferrins: Crystal structure of the open form of the N-terminal half-molecule of human transferrin. *Biochemistry 37*:13978–13986.

Kraulis P. 1991. MOLSCRIPT, a program to produce both detailed and schematic plots of protein structures. *J Appl Crystallogr 24*:946–950.

Laskowski RA, MacArthur MW, Moss DS, Thornton JM. 1993. PROCHECK: A program to check the stereochemical quality of protein structures. *J Appl Crystallogr 26*:283–291.

Li Y, Harris WR, Maxwell A, MacGillivray RTA, Brown T. 1998. Kinetic studies on the removal of iron and aluminum from recombinant and site-directed mutant N-lobe half transferrins. *Biochemistry 37*:14157–14166.

Lin LN, Mason AB, Woodworth RC, Brandts JF. 1993. Calorimetric studies of the N-terminal half-molecule of transferrin and mutant forms modified near the Fe^{3+}-binding site. *Biochem J 293*:517–522.

Luck LA, Mason AB, Savage KJ, MacGillivray RTA, Woodworth RC. 1997. ^{19}F NMR studies of recombinant human transferrin N-lobe and three single point mutants. *Magn Reson Chem 35*:477–481.

MacGillivray RTA, Moore SA, Chen J, Anderson BF, Baker H, Luo Y, Bewley M, Smith CA, Murphy MEP, Wang Y, et al. 1998. Two high-resolution crystal structures of the recombinant N-lobe of human transferrin reveal a structural change implicated in iron release. *Biochemistry 37*:7919–7928.

Mason AB, He QY, Tam BM, MacGillivray RTA, Woodworth RC. 1998. Mutagenesis of the aspartic acid ligands in human serum transferrin: Lobe–lobe interaction and conformation as revealed by antibody, receptor-binding and iron-release studies. *Biochem J 330*:35–40.

Mason AB, Woodworth RC, Oliver RWA, Green BN, Lin LN, Brandts JF, Tam BM, Maxwell A, MacGillivray RTA. 1996. Production and isolation of the recombinant N-lobe of human serum transferrin from the methylotrophic yeast *Pichia pastoris*. *Protein Expr Purif 8*:119–125.

McRee DE. 1992. A visual protein crystallographic software system for X11/XView. *J Mol Graphics 10*:44–46.

Merritt EA, Murphy MEP. 1994. Raster3d version 2.0. A program for photorealistic molecular graphics. *Acta Crystallogr D50*:869–873.

Otwinowski Z, Minor W. 1997. Processing of X-ray diffraction data collected in oscillation mode. *Methods Enzymol 276*:307–326.

Steinlein LM, Graf TN, Ikeda RA. 1995. Production and purification of N-terminal half-transferrin in *Pichia pastoris*. *Protein Expr Purif 6*:619–624.

Steinlein LM, Ligman CM, Kessler S, Ikeda RA. 1998. Iron release is reduced by mutations of lysines 206 and 296 in recombinant N-terminal half-transferrin. *Biochemistry 37*:13696–13703.

Wang Y, Chen J, Luo Y, Funk WD, Mason AB, Woodworth RC, MacGillivray RTA, Brayer GD. 1992. Preliminary crystallographic analyses of the N-terminal lobe of recombinant human serum transferrin. *J Mol Biol 227*:575–576.

Woodworth RC, Mason AB, Funk WD, MacGillivray RTA. 1991. Expression and initial characterization of five site-directed mutants of the N-terminal half-molecule of human transferrin. *Biochemistry 30*:10824–10829.

Zak O, Aisen P, Crawley JB, Joannou CL, Patel KJ, Rafiq M, Evans RW. 1995. Iron release from recombinant N-lobe and mutants of human transferrin. *Biochemistry 34*:14428–14434.

Zak O, Tam B, MacGillivray RTA, Aisen P. 1997. A kinetically active site in the C-lobe of human transferrin. *Biochemistry 36*:11036–11043.